Dynamic Behavior of Fluttering Two-Dimensional Panels on an Airplane in Pull-Up Maneuver

Slobodan R. Sipcic*
Boston University, Boston, Massachusetts 02215
and
Luigi Morino†
University of Rome "La Sapienza," Rome 00184, Italy

The governing equations, derived using Lagrangian mechanics, include geometric nonlinearities associated with the occurrence of tensile stresses, as well as coupling between the angular velocity of the maneuver and the elastic degrees of freedom. Longtime histories, phase plane plots, and power spectra of the response are the dynamics tools used in studying the system considered here. The effect of the maneuver on the flutter speed and on the amplitude of the limit cycle are presented for different load conditions. A new type of limit cycle has been observed for the nonmaneuvering case. It is also shown that the presence of a maneuver can transform the panel response from a fixed point into a simple periodic or even chaotic state. It can also suppress the periodic character of the motion, transforming the response into a fixed point. For a prescribed time-dependent maneuver, a remarkable response transition between the different types of limit cycles is presented.

Nomenclature

a = plate length
a_r = u_r/h
D = plate-bending stiffness
E = modulus of elasticity
$\mathcal{E}$ = elastic energy
g = acceleration due to gravity
h = plate thickness
j_1, j_2, j_3 = base vectors of the body frame of reference
K = spring constant
M = Mach number
N_x = applied in-plane force
n = $1+\omega v_0/g$
P = $\Delta p a^4/Dh$
$p-p_\infty$ = aerodynamic pressure
Q_r = generalized Lagrangian forces
q = $\rho v_0^2/2$
$\boldsymbol{R}$ = rotation matrix
R_x = $N_x a^2/D$
$\mathfrak{I}$ = kinetic energy
t = time
u = plate deflection
$\boldsymbol{u}$ = displacement of the structure
u_r = modal amplitude
v_0 = velocity
x = coordinates in the inertial frame of reference
z = coordinates in the body frame of reference
α = $Ka/(Ka+Eh)$
β = $\sqrt{M^2-1}$
λ = $2qa^3/\beta D$
μ = $\rho a/\rho_m h$
ν = Poisson's ratio
ξ^α = material coordinates
ρ = air density
ρ_m = plate density
τ = $t\sqrt{D/\rho_m h a^4}$
Φ_r = prescribed functions
ϕ_r = $\sin(r\pi z/a)$
ω = angular velocity
Ω = $\omega a/v_0$
$\boldsymbol{\Omega}$ = skew-symmetric matrix form of the angular velocity

I. Introduction

THIS paper deals with the dynamic behavior of a fluttering panel on a maneuvering airplane. Such a system is interesting from the dynamic point of view because it combines a maneuver (which manifests itself as forced excitations, as well as more complicated coupling, including parametric excitation) and flow-induced oscillations on a system with two fixed points (buckled plate). As a result of combining the force-induced and flow-induced oscillations, this system is a rich source of static and dynamic instabilities and of associated

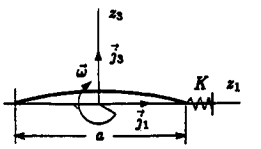

Buckled plate of a maneuvering airplane

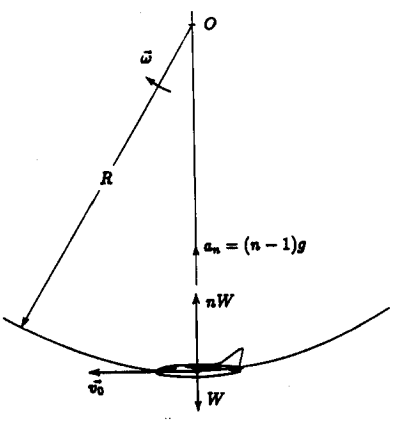

Fig. 1 Airplane in a pull-up.

Received March 1, 1990; revision received Sept. 15, 1990; accepted for publication Sept. 21, 1990.

*Assistant Professor, Department of Aerospace and Mechanical Engineering, 110 Cummington St. Member AIAA.
†Professor of Aeroelasticity, Dipartmento di Meccanica e Aeronautica, Via Eudossiana 18. Member AIAA.

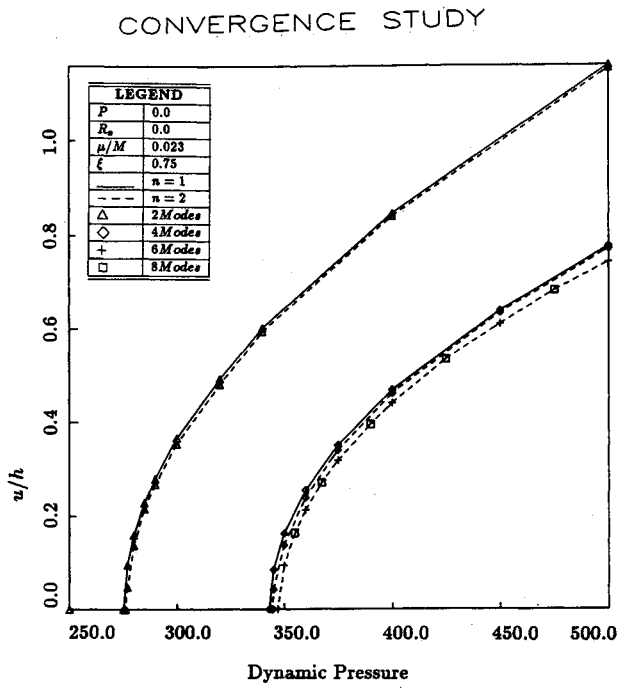

Fig. 2 Influence of the number of modes on panel response.

limit-cycle motions. In the past, several approaches have been used in the treatment of these two problems. Very simple models have been used for the simple problem of forced vibration of a buckled plate (essential to the understanding of the more complicated system under consideration, Dowell and Ilgamov[1]). For example, in Dowell and Pezeshki,[2,3] Zavodney and Nayfeh,[4] or Zavodney et al.,[5] Duffing's equation has been used as a model for the sinusoidally excited buckled plate. For the problem under consideration, the nonlinear partial differential equation is approximated, by Galerkin or Rayleigh-Ritz methods, as a set of ordinary differential equations that are then solved for specific initial conditions by numerical integration techniques. An excellent review of the work using this approach is given in Dowell and Ilgamov.[1] Note that a related problem is studied by Holmes and Marsden,[6] who presented one of the very few analytical results available on chaos in a continuous system.

We are interested here with highly maneuverable aircraft. One feature of thes aircraft is that the angular velocity can be much higher than in more conventional aircraft. As a consequence, a body frame of reference connected with the aircraft cannot be assumed to be in pure translation, and the equations should be written in a rotating frame of reference. This implies that there is a coupling between the rigid-body and the flexible-body motion. Note that the effect of maneuvering on the dynamic response of a fluttering panel is not discussed by Dowell and Ilgamov.[1] This effect was analyzed by Sipcic and Morino.[7] A portion of their work is summarized here. The chaotic response is studied in much more detail in the original work, and will be the subject of a subsequent paper.

This paper has been divided into two main areas, theoretical and numerical. Assuming that the aircraft maneuver is prescribed, the Lagrange equations of motion for the elastic degrees of freedom are derived in Sec. II. These are the governing equations for the physical system considered here. Numerical results are presented in Sec. III. The governing equations are integrated numerically, using a fourth-order Runge-Kutta algorithm. To understand the dynamic problem, the character of the solution has been examined in Sec. III.B in physical terms. The effect of varying the load factor was studied in great detail; but only representative results are presented in Secs. III.C–III.F. Finally, a time-dependent maneuver is considered in Sec. III.G.

II. Equation of Motion

Consider a thin, two-dimensional, simply supported plate having length a, thickness h, and undergoing cylindrical bending in response to one-sided airflow (see Fig. 1). As previously mentioned, the plate motion is expressed in terms of the rigid-body translation and rotation of the body reference frame, and a deformation. Indicating the coordinates in the inertial frame with x, the coordinates of the origin P_0 of the body frame with x_0, the body-axis coordinates of a point P in the body frame at time $t=0$ (reference condition) with z, and the body-axis components of the displacement of the structure with respect to a reference condition with u, we have

$$x(\xi^\alpha,t) = x_0(t) + R(t)\left[z(\xi^\alpha) + u(\xi^\alpha,t)\right] \tag{1}$$

where ξ^α is a system of material coordinates (i.e., a system of coordinates, in general, curvilinear; that is, convected with the material point). Typically, these coincide numerically with the components z_i of z. Note that the matrix R represents a rigid-body rotation. Next, let us assume that a deformation is given

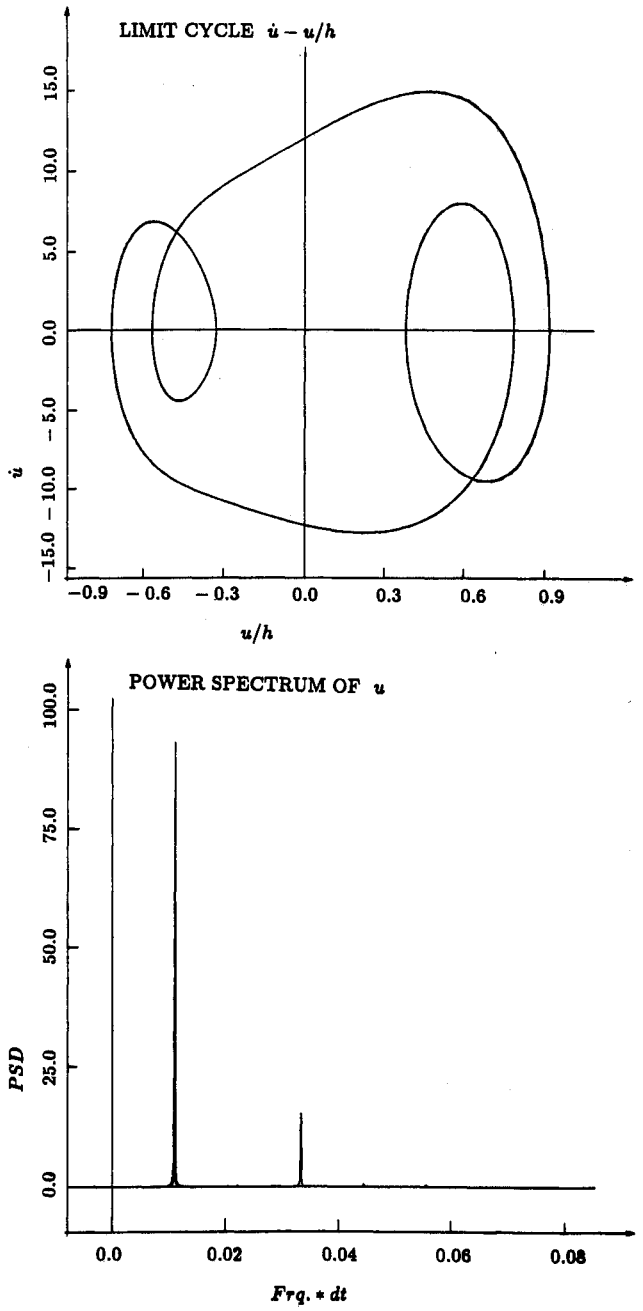

Fig. 3a Character of the response without maneuvering ($n = 1.00$).

as a linear combination of prescribed functions Φ_r with unknown coefficients u_r $(r=1,\ldots,N)$, i.e.,

$$u(\xi^\alpha,t)=\sum_r u_r(t)\Phi_r(\xi^\alpha) \tag{2}$$

In what follows, the equations of motion for the elastic degrees of freedom u_r are obtained by the use of Lagrange's equations in the form

$$\frac{\mathrm{d}}{\mathrm{d}t}\frac{\partial \mathfrak{I}}{\partial \dot{u}_r}-\frac{\partial \mathfrak{I}}{\partial u_r}+\frac{\partial \mathfrak{E}}{\partial u_r}=Q_r \tag{3}$$

A. Kinetic Energy

The kinetic energy is given by

$$\mathfrak{I}=\frac{1}{2}\iiint_V \rho_m \|v\|^2\,\mathrm{d}V \tag{4}$$

The velocity v of a point ξ^α may be obtained from Eq. (1), as

$$v(\xi^\alpha,t)=\left.\frac{\partial x}{\partial t}\right|_{\xi^\alpha}=\dot{x}_0(t)$$
$$+R(t)\left\{\Omega(t)\left[z(\xi^\alpha)+u(\xi^\alpha,t)\right]+\dot{u}(\xi^\alpha,t)\right\} \tag{5}$$

where Ω is the skew-symmetric matrix form of the angular velocity, and $\dot{x}_0(t)$ is the velocity v_0 of the origin P_0, with respect to the inertial frame of reference.

In what follows, a constant velocity pull-up maneuver will be assumed. If the base vectors of the body frame of reference are j_1, j_2, j_3 (see Fig. 1), then $v_0=-v_0 j_1$ and the angular velocity $\omega=-\omega j_2$. Furthermore, the prescribed functions Φ_r are all in the direction j_3. Making use of these assumptions,

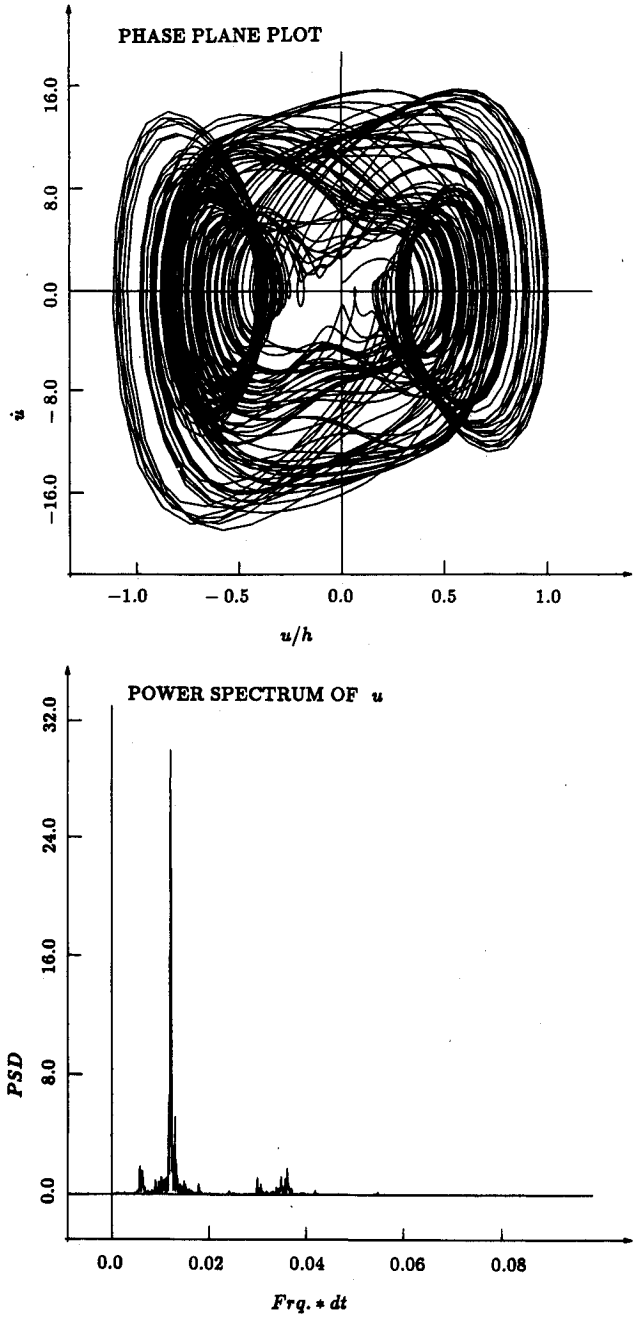

Fig. 3b Character of the response with maneuvering ($n=1.28$).

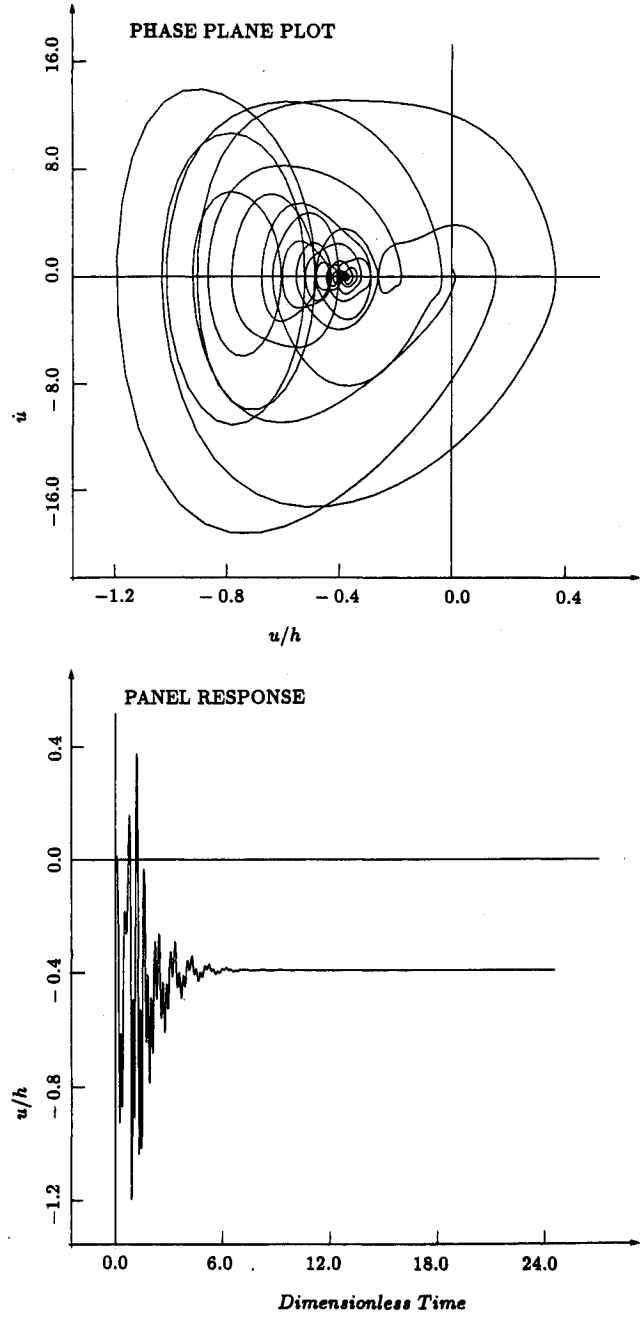

Fig. 3c Character of the response with maneuvering ($n=3.00$).

and substituing Eqs. (2) and (5) into Eq. (4), it is found that

$$\mathfrak{I} = \frac{1}{2} m v_0^2 + \frac{1}{2}\omega^2 \sum_{r,s} m_{rs} u_r u_s - v_0 \omega \sum_r s_r u_r + \frac{1}{2}\omega^2 J_0 + \frac{1}{2}\sum_{r,s} m_{rs}\dot{u}_r\dot{u}_s + \omega \sum_r b_r \dot{u}_r \tag{6}$$

where

$$m = \iiint_V \rho_m \, dV, \qquad m_{rs} = \iiint_V \rho_m \phi_r \phi_s \, dV$$

$$b_r = \iiint_V \rho_m z \phi_r \, dV, \qquad s_r = \iiint_V \rho_m \phi_r \, dV$$

$$J_0 = \iiint_V \rho_m z^2 \, dV \tag{7}$$

Substituting Eq. (6) into Eq. (3), the equations of motion become

$$s_r \omega v_0 + b_r \dot{\omega} + \sum_s m_{rs}\ddot{u}_s - \omega^2 \sum_s m_{rs} u_s + \frac{\partial \mathcal{E}}{\partial u_r} = Q_r \tag{8}$$

B. Elastic Energy

Consider once more a thin, two-dimensional, simply supported plate having length a and thickness h and undergoing cylindrical bending in response to one-sided airflow (see Fig. 1). In such a case, the axial extension v can be written to first-order approximation as

$$v(z) = -\frac{1}{2}\int_0^z \left(\frac{\partial u}{\partial z}\right)^2 dz \tag{9}$$

Thus, the elastic energy is

$$\mathcal{E} = \frac{D}{2}\int_0^a \left(\frac{\partial^2 u}{\partial z^2}\right)^2 dz + \frac{\alpha E h}{2a}\left[\frac{1}{2}\int_0^a \left(\frac{\partial u}{\partial z}\right)^2 dz\right]^2 \tag{10}$$

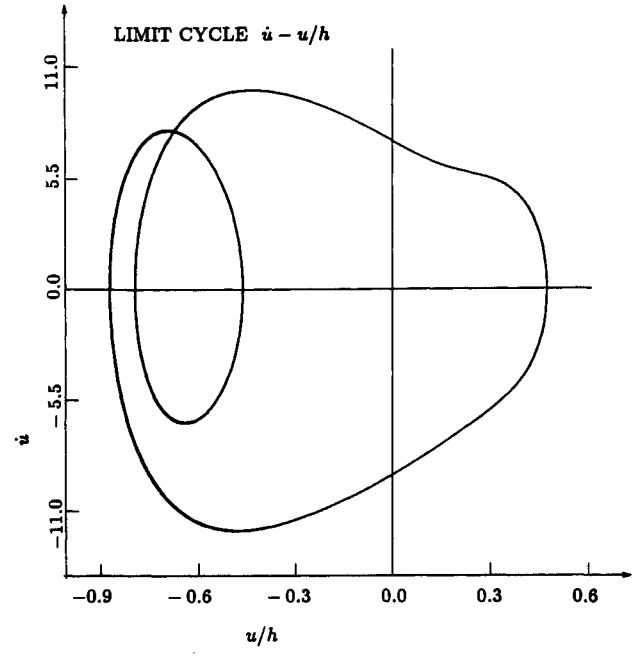

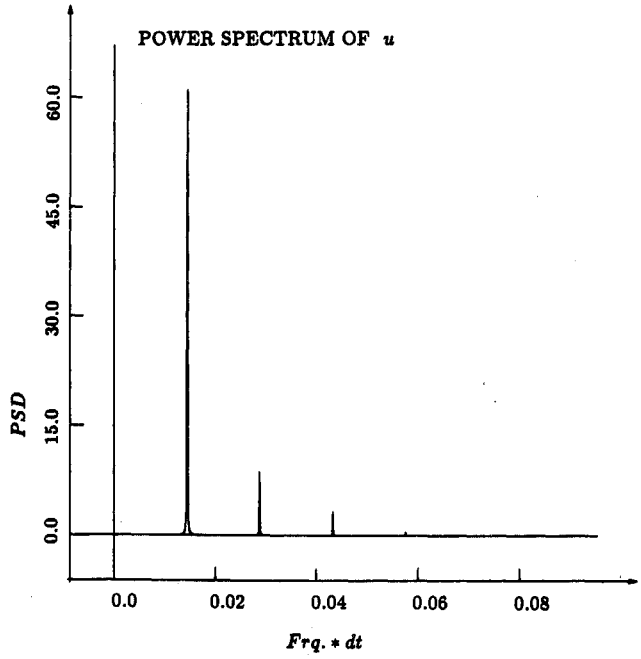

Fig. 3d Character of the response with maneuvering ($n = 1.67$).

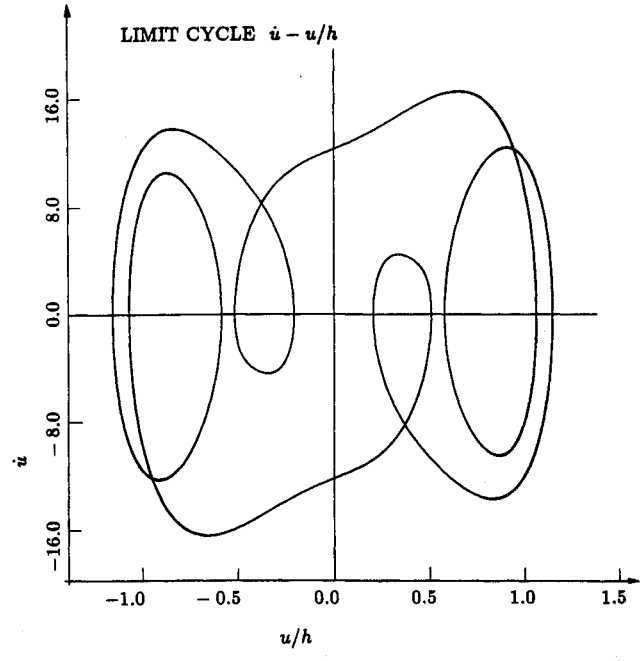

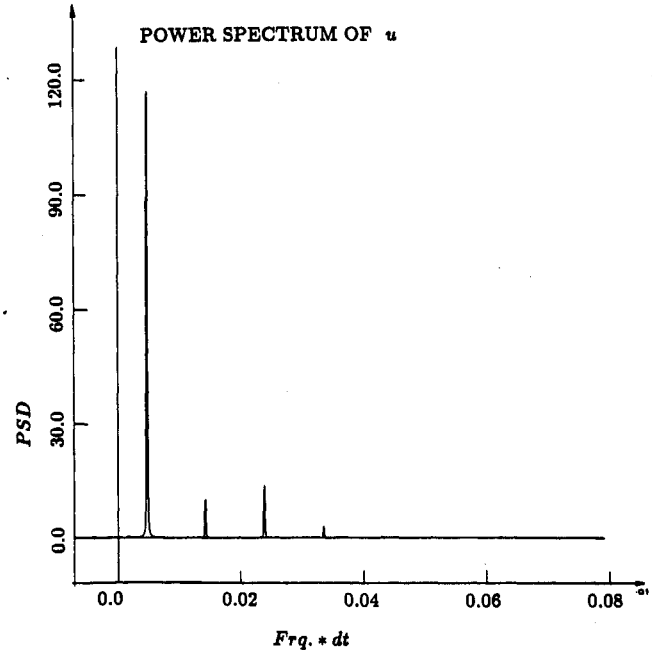

Fig. 4 Panel response for $n = 1.00$, $\lambda = 119.5$, and $R_x = -4.0\pi^2$.

where D is a plate bending stiffness, α is a support factor accounting for the effective stiffness of the supporting structure defined by

$$\alpha = \frac{Ka}{Ka + Eh} \tag{11}$$

and K is a spring constant per unit spanwise length of panel. Substituting Eq. (2) into the elastic energy, Eq. (10), and differentiating with respect to u_r, one obtains

$$\frac{\partial \mathcal{E}}{\partial u_r} = D \sum_s e_{rs} u_s + \frac{\alpha Eh}{2a} \sum_s \sum_m \sum_l k_{rsml} u_s u_m u_l \tag{12}$$

where

$$k_{rsml} = \int_0^a \phi_s' \phi_m' \, dz \int_0^a \phi_l' \phi_r' \, dz$$

$$e_{rs} = \int_0^a \phi_s'' \phi_r'' \, dz \tag{13}$$

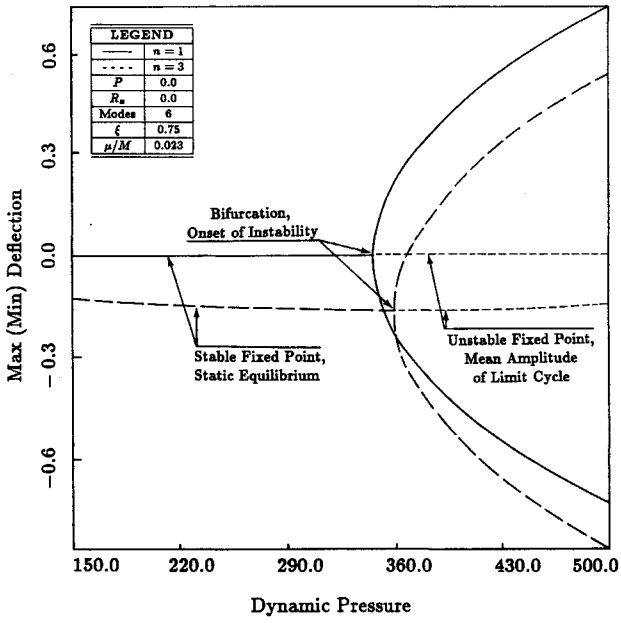

Fig. 5 Effect of load factor on the panel response.

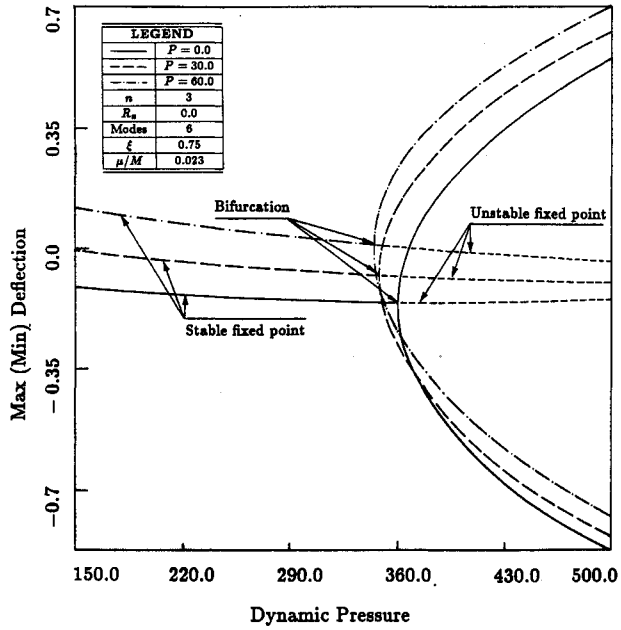

Fig. 6 Influence of static pressure differential on the panel response.

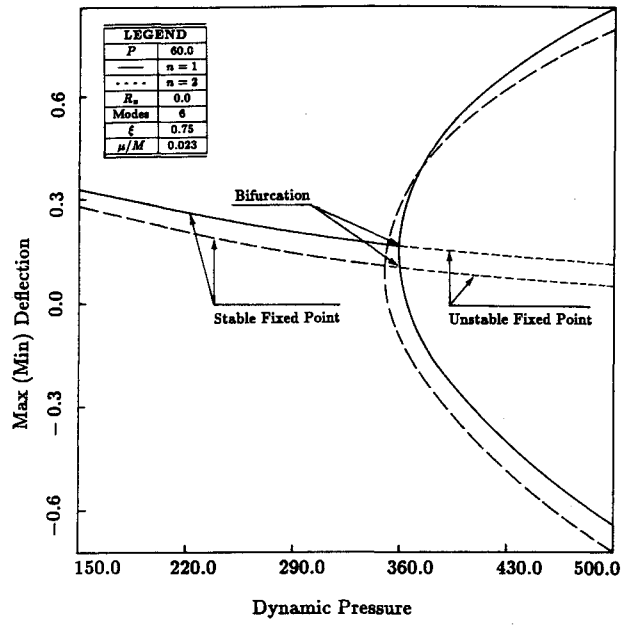

Fig. 7 Combined influence of maneuvering and static pressure differential on the panel response.

C. Generalized Lagrangian Forces

Assume that the plate is exposed to an in-plane tensile load N_x and to a static pressure difference across the plate ΔP, and that the exciting dynamic pressure difference is given by quasi-steady aerodynamic theory, i.e.,[8]

$$p - p_\infty = \frac{2q}{\beta} \left[\frac{\partial u}{\partial z} + \frac{M^2 - 2}{M^2 - 1} \frac{1}{v_0} \frac{\partial u}{\partial t} \right] \tag{14}$$

Following the conventional procedure of Lagrangian mechanics, i.e., calculating the virtual work performed by the external forces as they act through the virtual displacement caused by the variation in the generalized coordinate u_r, the expression for the generalized force Q_r is

$$Q_r = -N_x \sum_s n_{rs} u_s + \Delta P p_r - \frac{2q}{\beta} \sum_s (u_s p_{rs} + \dot{u}_s \hat{p}_{rs}) \tag{15}$$

where

$$n_{rs} = \int_0^a \phi_r' \phi_s' \, dz, \qquad p_r = \int_0^a \phi_r \, dz$$

$$p_{rs} = \int_0^a \phi_r \phi_s' \, dz, \qquad \hat{p}_{rs} = \frac{\beta^2 - 1}{\beta^2 v_0} \int_0^a \phi_r \phi_s \, dz \tag{16}$$

Substituting Eqs. (12) and (15) into the equations of motion (8), one obtains

$$s_r \omega v_0 + b_r \dot{\omega} + \sum_s m_{rs} \ddot{u}_s - \omega^2 \sum_s m_{rs} u_s + D \sum_s e_{rs} u_s + \frac{\alpha Eh}{2a} \sum_s \sum_m \sum_l k_{rsml} u_s u_m u_l + N_x \sum_s n_{rs} u_s + \frac{2q}{\beta} \sum_s (u_s p_{rs} + \dot{u}_s \hat{p}_{rs}) = \Delta P p_r \tag{17}$$

D. Dimensionless Equations

In order to recast Eq. (17) in a dimensionless form, we introduce the following dimensionless parameters and coordinates:

$$a_r = \frac{u_r}{h}, \qquad \tau = t \left(\frac{D}{\rho_m h a^4} \right)^{1/2}, \qquad \Omega = \frac{\omega a}{v_0}, \qquad \lambda = \frac{2qa^3}{\beta D}$$

$$R_x = \frac{N_x a^2}{D}, \qquad P = \frac{\Delta P a^4}{Dh}, \qquad \mu = \frac{\rho a}{\rho_m h} \tag{18}$$

Furthermore, since the plate is simply supported, we will allow the prescribed functions to be

$$\phi_r = \sin(r\pi z/a) \tag{19}$$

Substiuting Eq. (19) into Eqs. (7), (13), and (16), and, thence, into Eq. (17), the equation of motion in dimensionless form reads

$$\ddot{a} + \delta\dot{a} + Ga + f(a) + \gamma\Omega^2 a = p + \dot{\Omega}d + \Omega v \tag{20}$$

where $a = \{a_r\}$, $G = [g_{rs}]$, $d = \{d_r\}$, $v = \{v_r\}$, $p = \{p_r\}$, $f = \{f_r\}$, and

$$g_{rs} = 2\lambda\frac{rs}{r^2 - s^2}\left[1 - (-1)^{r+s}\right] + \left[(r\pi)^2 R_x + (r\pi)^4\right]\delta_{rs}$$

$$\delta = \frac{\beta^2 - 1}{\beta^2}\left(\frac{\lambda\mu}{M}\right)^{1/2}, \qquad d_r = -2\frac{(-1)^r}{\pi r}\left(\frac{\beta\lambda}{\mu}\right)^{1/2}\frac{a}{h}$$

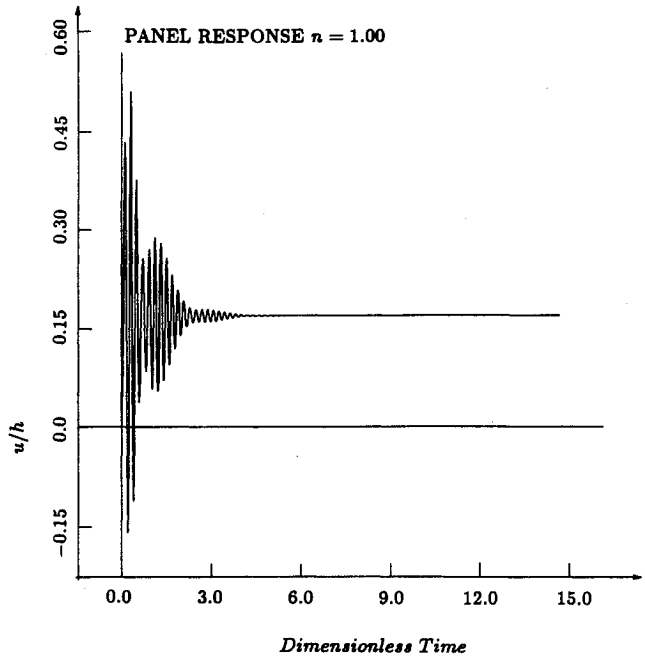

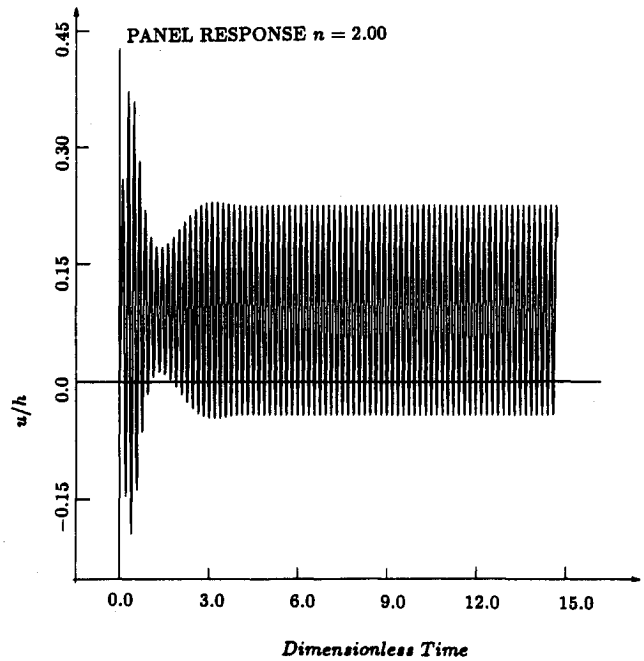

Fig. 8 Panel response for $\lambda = 355$, $R_x = 0.0$, and $P = 60.0$.

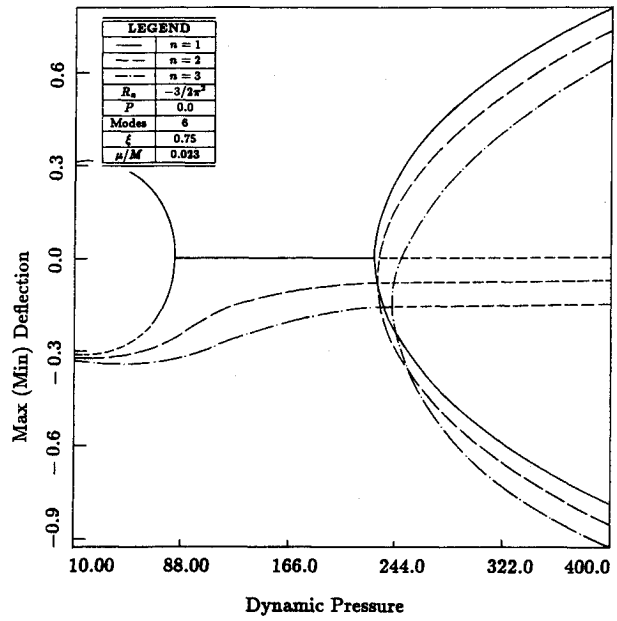

Fig. 9 Combined influence of maneuvering and in-plane loading on the panel response.

$$v_r = -2\frac{\beta\lambda}{\mu}\frac{a}{h}\frac{\left[1-(-1)^r\right]}{\pi r}, \qquad p_r = 2P\frac{\left[1-(-1)^r\right]}{\pi r}$$

$$\gamma = -\frac{\beta\lambda}{\mu}, \qquad f_r = 3r^2\pi^4\alpha(1-\nu^2)a_r\sum_s s^2 a_s^2 \tag{21}$$

with $s, r = 1, \ldots, N$. Equations (20) are a set of ordinary nonlinear differential equations in time. The cubic nonlinearities are of geometric origin and are associated with the occurrence of tensile stresses in the middle surface. The coupling between the rigid-body rotation of the frame of reference and the elastic degrees of freedom is represented by the fifth term. This set of equations has been solved by a direct numerical integration. Note that by assuming $\Omega = 0$, Eqs. (20) properly reduce to the classical panel flutter equations (see, e.g., Bolotin,[9] or Dowell[10]).

III. Numerical Experimentation

In this research, numerical simulations are conducted to analyze the behavior of a fluttering panel on a maneuvering airplane. Equations (20) are simulated on the digital computer using a fourth-order Runge-Kutta algorithm. For the sake of clarity, the factor Ω is expressed in terms of the load factor $n = 1 + \omega v_0/g$, as $\Omega = (n-1)ag/v_0^2$. The load factor for aeronautical applications is in the range 1-6. For all of the results reported here, $\mu/M = 0.023$, $\alpha = 1$, $\nu = 0.3$, $h/a = 0.008$, $M = 1.3$, $ag/v_0^2 = 1.45 \times 10^{-5}$, and the plate response is calculated at $z/a = 0.75$. To eliminate the influence of the initial conditions from the maneuvering, the same initial conditions are prescribed for all cases by setting $\dot{a}_1 = 1.0$ (corresponding to a positive velocity of the first degree of freedom).

A. Convergence

The effect of the number of degrees of freedom (i.e., number of modes) used in the analysis is an important parameter. Therefore, a comparison is made for the load factor $n = 2$ in Fig. 2, where the plate amplitude of the limit cycle is given as a function of λ for $P = 0.0$, $R_x = 0.0$ for 2, 4, 6, and 8 modes. The solution appears to have converged for six modes of freedom, whereas with only two modes the results are inaccurate. Also shown in Fig. 2 are nonmaneuvering results for 2 and 4 modes. Similar behavior of the convergence process is evident. Since the solution has converged for six modes, all the subse-

quent computations presented here have been performed using six degrees of freedom.

B. Character of the Solution in the Presence of a Maneuver

For the sake of clarity, before addressing the general results, the key types of responses are introduced from a physical point of view. The buckled plate is on the upper side of the wing of a maneuvering airplane (see Fig. 1), and is being excited by the airflow over its upper surface. Depending on the value of the load factor and other parameters, one or two fixed points may be obtained. The first fixed point corresponds to the undeformed position, the other two to the up-buckled or down-buckled plate positions. The plate motion, generally speaking, consists of vibration around up-buckled, down-buckled positions, and "snapping through" motion. Finally, there is also the possibility of a chaotic response.

Figure 3 shows selected phase-plane plots of the panel response, as well as their power spectrum estimates. For the base case of $\lambda = 150$, and $R_x = -3.0\pi^2$, maneuver at various loads factors were studied. Figure 3a corresponds to a nonmaneuvering case. The motion has nonchaotic character, with three orbits in evidence. One may think of this as the sequence of the plate vibration around up-buckled position, snapping through followed by vibration about the down-buckled position. A load factor $n = 1.28$ transforms the response into a chaotic state (see Fig. 3b), whereas a load factor $n = 3$ suppresses the periodic character of the motion, the response is a fixed point, and all motion ceases (see Fig. 3c). An equally interesting result occurs at $n = 1.67$, when the inertial forces due to the maneuver have suppressed the plate vibration around the up-buckled position (see Fig. 3d).

With the in-plane load $R_x = -4.0\pi^2$, and with the velocity parameter between $\lambda = 119.275$ and $\lambda = 120.496$, a new limit cyle of the form presented in the Fig. 4 has been found for the nonmaneuvering base case with $n = 1$.

C. Effect of Load Factor

In Fig. 5, the effect of the pull-up maneuver on the maximum and minimum values of the plate defleciton is shown. To eliminate the influence of the static pressure differential, and

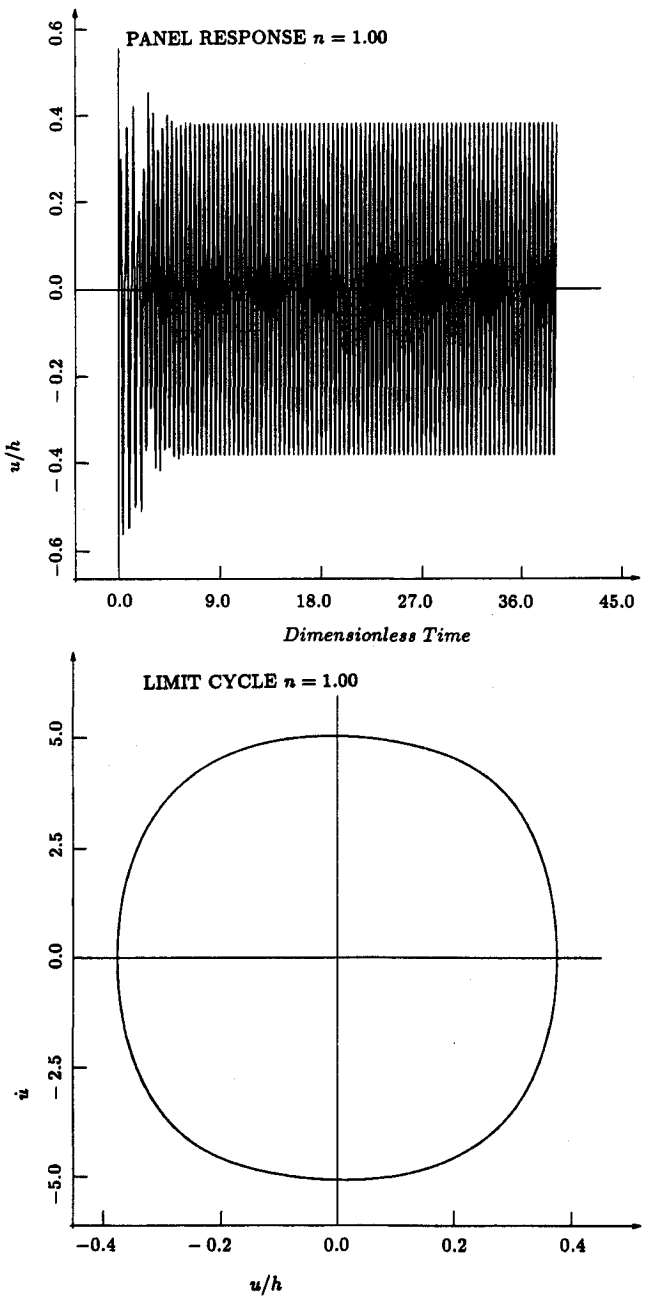

Fig. 10a Panel response for $P = 0.0$ and $R_x = -3.0\pi^2$, without maneuvering ($n = 1.00$).

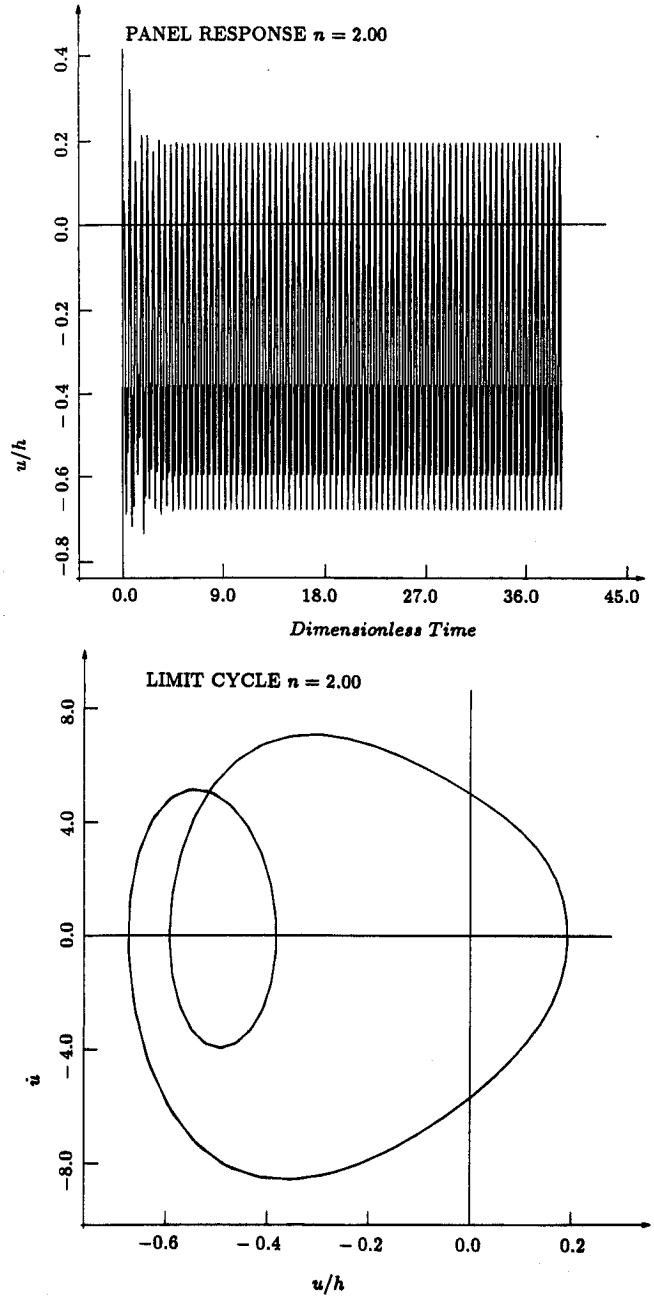

Fig. 10b Panel response for $P = 0.0$, $R_x = -3.0\pi^2$, and constant velocity pull-up maneuver ($n = 2.00$).

in-plane loading, we have set $P=0.0$ and $R_x=0.0$. In the absence of the static pressure differential and inertial forces due to the maneuver, the undeformed plate position is the statically stable case $n=1$ in Fig. 5. In the maneuvering case, the plate deforms to some static equilibrium position under the inertial forces, due to the maneuver (see Fig. 5 for $n=3$). For sufficiently large flow velocity, this equilibrium position becomes unstable. In the nonmaneuvering case ($n=1$), the change in the nature of the stable solution, through a supercritical or normal bifurcation, occurs for the critical parameter value $\lambda_c=342.2$. The new simple harmonic limit cycle motion with a zero amplitude at the bifurcation point is created. Similarly, in the case of the maneuver $n=3$, the solution bifurcates for $\lambda_c=359.5$. It is apparent that the flutter speed increases with n (i.e., the linear solution is stabilized by the presence of the load factor). Secondly, the inertial forces, due to the maneuver, increase the static plate deflection (negative, in this case), as well as the mean amplitude of a limit cycle motion.

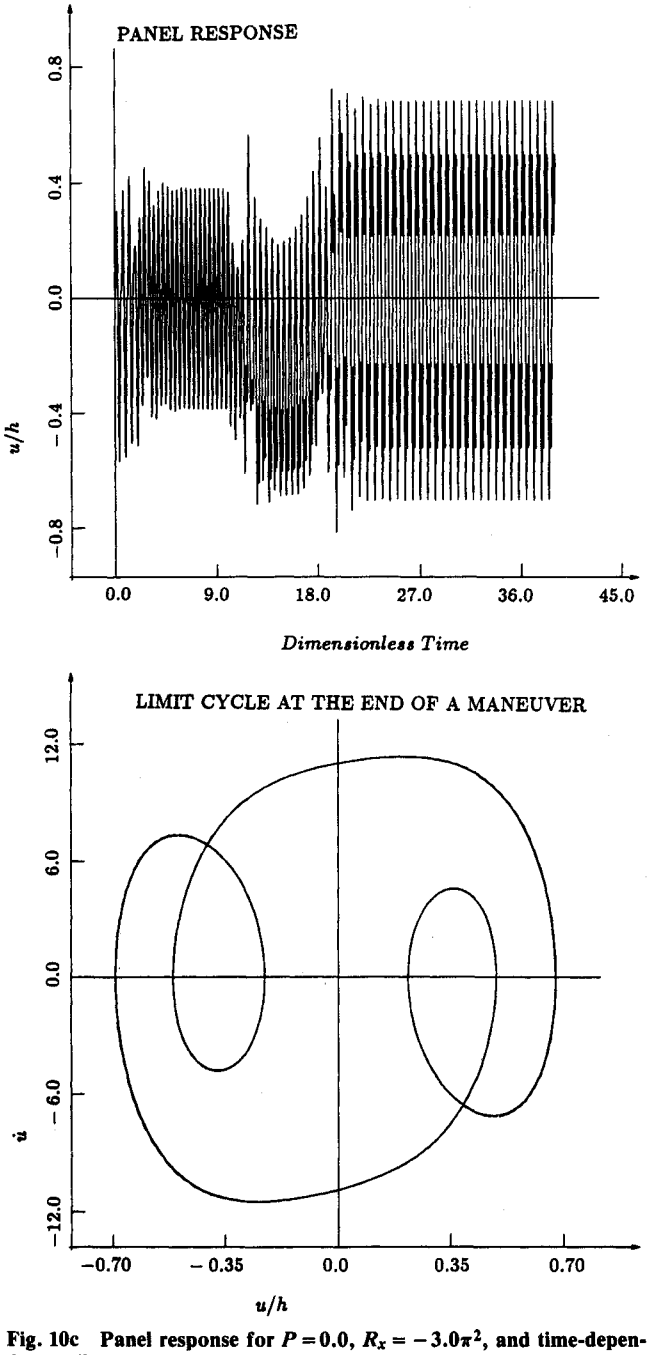

Fig. 10c Panel response for $P=0.0$, $R_x=-3.0\pi^2$, and time-dependent pull-up maneuver (amplitude $n=2.00$).

For relatively large n, the inertial forces will suppress the periodic character of the motion, transforming the response into a fixed point; the given flow velocity is not large enough to disturb the static equilibrium shape (see also Fig. 3c).

D. Effect of Static Pressure Differential

The effect of the static pressure differential on the panel response, for a given load factor $n=3$, is presented in Fig. 6. The maximum and minimum values of the plate deflection are plotted as a function of the dynamic pressure λ for several pressure differentials P. In the absence of a static pressure differential, the plate deforms to some static equilibrium position under the inertial forces due to the maneuver (see Fig. 6 for $P=0.0$). Since the static pressure and inertial forces act in opposite directions, the static pressure differential decreases this initial deformation (i.e., makes it less negative) (see Fig. 6 for $P=30$ or $P=60$). The change in the nature of the stable solution, through a supercritical bifurcation, occurs for the critical parameter value $\lambda_c=359.5$, 346.0, and 341.7 for the loading conditions $P=0.0$, 30, and 60, respectively. Contrary to the influence of the maneuvering, the flutter speed decreases with increasing static pressure differential. Note that the load factor is related with the static pressure differential P, and analysis of their simultaneous influence on the panel response is in order.

E. Combined Influence of Maneuvering and Static Pressure Differential

In Fig. 7, the influence of a maneuver on the maximum and minimum values of the plate deflection is shown for the static pressure differential $P=60$. As previously mentioned, the inertial forces, due to a maneuver, decrease the plate deformation caused by the static pressure differential. For the critical value of the parameter $\lambda=361$ in the nonmaneuvering case and $\lambda=353$ in the maneuvering case, a supercritical bifurcation occurs. In each case, the fixed point in the parameter space bifurcates, and a new simple harmonic limit cycle motion, with zero amplitude at the bifurcation point, is created. Note that in the range $\lambda=353$–361, the occurrence of a maneuver changes the character of the response in the phase space from a fixed point ($n=1$) to a limit cycle ($n=2$). This is further illustrated in Fig. 8, where the plate time responses are given for $\lambda=355$. In the nonmaneuvering $n=1$ case, the response is a fixed point, whereas in the maneuvering $n=2$ case, the response is a simple periodic.

F. Effect of In-Plane Loading

The combined influence of a maneuver and an in-plane loading has also been studied. The results are presented in Fig. 9. The plate amplitude is shown vs dynamic pressure λ for several load factors $n=1$, 2, and 3 and in-plane load $R_x=-3/2\pi^2$.

For small λ, there are two branches to the curve associated with buckled configurations. Depending on the initial conditions, either one of these equilibrium positions is possible. While maneuvering, the upper buckled position appears only for very small λ. With increasing λ, for a given $R_x=-3/2\pi^2$, the solution is a stable fixed point in the parameter space. The change in the nature of the stable solution, through a supercritical bifurcation, occurs for the critical parameter value $\lambda_c=228$, 230, and 233 for the maneuvering conditions $n=1$, 2, and 3, respectively. It is apparent that increasing the load factor is related to increasing the critical parameter value λ at the bifurcation point.

G. Nonautonomous Equations

In all the results presented, we have considered a constant radius pull-up (with gravity parallel to the inertial load, i.e., for the aircraft at the bottom of the pull-up). The transient response at the beginning of a pull-up maneuver is considered here. In the case in which the angular velocity is given as

function of time, the differential equations (20) are nonautonomous. Consider an airplane in a pull-up maneuver during the time interval (t_1, t_2). The angular velocity is given by $\omega = \omega_0 \sin[\alpha(t - t_1)]$, with $\alpha = \pi/(t_2 - t_1)$. Under these assumptions, the angular velocity at the beginning and at the end of the maneuver is equal to zero. For the case of $\lambda = 150$ and $R_x = -3.0\pi^2$, the nonmaneuvering $n = 1.00$ response of the plate is a simple harmonic (see Fig. 10a). A constant velocity pull-up maneuver at $n = 2.00$ transforms this response into a more complicated limit cycle with two orbits (see Fig. 10b). Now consider a sinusoidal maneuver with the amplitude $n = 2.00$. As might be expected on physical grounds, our calculations show a disturbance of the simple harmonic limit cycle by the inertial forces, due to maneuvering. The remarkable results appear after the completion of the maneuver, when the panel motion is a more complicated limit cycle with three closed orbits in evidence (see Fig. 10c). To understand this result, note that the conditions at the end of the maneuver correspond to the initial conditions for the nonmaneuvering continuation of the flight. It is then apparent that the presence of maneuvering has moved the initial conditions into a basin of the attraction of the new attractor. In some regions of the initial condition space, one may expect even more dramatic changes of the dynamical behavior, due to time-dependent maneuver, especially close to the boundaries of the basin of attraction. It is clear that this study has to be related to the analysis of the influence of initial conditions. This may be a subject of future research.

IV. Concluding Remarks

A general geometrically exact Lagrangian mechanics formulation for the aeroelastic analysis of a maneuvering aircraft has been specialized to the case of a fluttering two-dimensional plate undergoing a pitching maneuver. The formulation includes the geometric nonlinearities associated with the occurrence of tensile stresses in the middle surface, as well as the effect of the rigid-body rotation on the other degrees of freedom. The general response of the system was simulated on a digital computer, using a fourth-order Runge-Kutta algorithm. Long-time histories, phase-plane plots, and power spectra have been used to characterize the response. A new type of limit cycle has been observed in the nonmaneuvering case. It was shown that chaos can occur during a maneuver for system parameters in the actual flight range. The presence of a maneuver load factor can transform the response from the fixed point into a simple periodic or even chaotic state. It can also suppress the periodic character of the motion, transforming the response into a fixed point, so that motion ceases.

The numerical experiments were performed with different time simulation lengths to ensure that the steady-state response has been reached and the transient has decayed. Furthermore, the computations were performed with various step sizes. The results were in good agreement and showed that for a sufficiently small time step, no numerical instability occurred and the results for the time simulation were closely reproducible.

The results indicate that the study of the deterministic system is important from the practical and theoretical viewpoint. First, the fact that a maneuver can change the character of the panel response is of practical interest to aeroelasticians, as it affects, for instance, fatigue analysis. Second, the techniques employed in this study can be extended to the problem of aeroelasticity of aircraft (with all nonlinearities—geometric, dynamic, and aerodynamic—included). From the theoretical point of view, this physical system is a rich source of static and dynamic instabilities and of associated limit-cycle motions, and it could be used, for instance, as a test case for assessing techniques for the study of nonlinear dynamics and chaos.

Subjects for consideration in future research include the use of other stability concepts, such as Lyapunov exponents and Poincaré maps. Application of complementary methods of differentiable dynamics—in particular, of center manifold and bifurcation theory—to analyze the problem from a qualitative viewpoint would be helpful. Knowledge of generic structures of attracting sets in N-space might make the interpretation of numerical solution of evolution equations considerably clearer.

Acknowledgments

Research was partially sponsored by the Air Force Office of Scientific Research under Contract F49620-86-C-0040. The authors wish to thank Anthony K. Amos of the Air Force Office of Scientific Research, Carey S. Buttrill of NASA Langley Research Center, and Guido Sandri of Boston University for valuable discussions on this work.

References

[1]Dowell, E. H., and Ilgamov, M., *Studies in Nonlinear Aeroelasticity,* Springer-Verlag, New York, 1988.

[2]Dowell, E. H., and Pezeshki, C., "On the Understanding of Chaos in the Duffing's Equation Including a Comparison with Experiment," *Journal of Applied Mechanics,* Vol. 52, March 1986, pp. 949–957.

[3]Pezeshki, C., and Dowell, E. H., "An Examination of Initial Condition Maps for the Sinusoidally Excited Buckled Beam Modeled by the Duffing's Equation," *Journal of Sound and Vibration,* Vol. 117, No. 2, 1987, pp. 219–232.

[4]Zavodney, L. D., and Nayfeh, A. H., "The Response of a Single-Degree-of-Freedom System With Quadratic and Cubic Non-Linearities to a Fundamental Parametric Resonance," *Journal of Sound and Vibration,* Vol. 120, No. 1, 1988, pp. 63–93.

[5]Zavodney, L. D., Nayfeh, A. H., and Sanchez, N. E., "The Response of a Single-Degree-of-Freedom System With Quadratic and Cubic Non-Linearities to a Principal Parametric Resonance," *Journal of Sound and Vibration,* Vol. 129, No. 3, 1989, pp. 417–442.

[6]Holmes, P. J., and Marsden, J., "A Partial Differential Equation with Infinitely Many Periodic Orbits: Chaotic Oscillations of a Forced Beam," *Archives for Rational Mechanics and Analysis,* Vol. 76, No. 2, 1981, pp. 135–166.

[7]Sipcic, R. S., and Morino, L., "Chaotic Response of Fluttering Panel, the Influence of Maneuvering," Boston Univ., Boston, MA, TR 89-1, Sept. 1989.

[8]Bisplinghoff, R. L., and Ashley, H., *Principles of Aeroelasticity,* Dover, New York, 1962.

[9]Bolotin, V. V., *Nonconservative Problems of the Theory of Elastic Stability,* Pergamon, London, 1963.

[10]Dowell, E. H., "Nonlinear Oscillations of a Fluttering Plate," *AIAA Journal,* Vol. 4, No. 7, 1966, pp. 1267–1276.